September 29, 2017

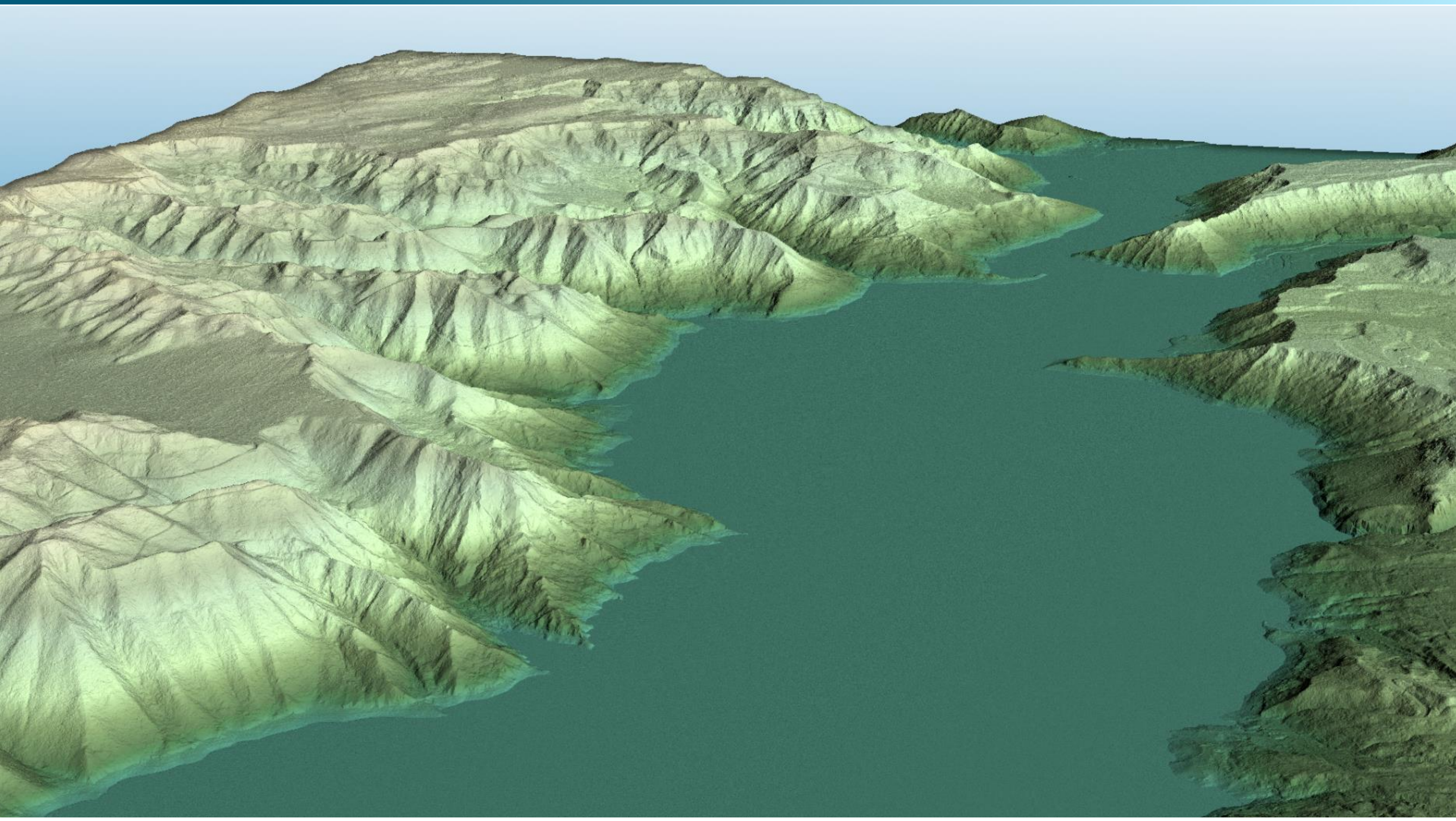

Western Washington 3DEP LiDAR Technical Data Report

Contract No. G16PC00016, Task Order No. G16PD00383

Amanda Lowe
USGS NGTOC
1400 Independence Rd. MS547
Rolla, MO 65401

QSI Corvallis
517 SW 2nd St., Suite 400
Corvallis, OR 97333
PH: 541-752-1204

Table of Contents

Cover Photo: A view looking north over Lake Shannon in the Western Washington 3DEP LiDAR project area.

INTRODUCTION

This photo taken by QSI acquisition staff shows a view of Colonial and Pyramid Peaks in Washington's North Cascade Mountains.

In March 2016, Quantum Spatial (QSI) was contracted by the United States Geological Survey (USGS), in collaboration with the Washington Department of Natural Resources (WADNR), to collect Light Detection and Ranging (LiDAR) data for the Western Washington 3DEP QL1 LiDAR project site in the state of Washington. The Western Washington 3DEP LiDAR project area covers approximately 3.5 million acres within portions of thirteen counties in the state of Washington; Whatcom, Skagit, Snohomish, Thurston, Lewis, Clark, Cowlitz, Wahkiakum, Skamania, and Grays Harbor. Data were collected to aid USGS in assessing the topographic and geophysical properties of the study area.

QSI provided the Northern portion of the Western Washington 3DEP project area to USGS on September 1st, 2017; this comprehensive report accompanies the Southern portion of the project area, which concludes the LiDAR processing deliveries to USGS for this project. Summarized herein are contract specifications, data acquisition procedures, processing methods, and analysis of the final dataset including LiDAR accuracy and density, for the entire Western Washington 3DEP project area. Acquisition dates and acreage are shown in Table 1, a complete list of contracted deliverables provided to USGS is shown in Table 2, and the project extent is shown in Figure 1.

Table 1: Acquisition dates, acreage, and data types collected on the Western Washington 3DEP site

Project Site	Total Acres	Acquisition Dates	Data Type
Western Washington 3DEP – North AOI	1,984,774	March 17th, 2016 – September 30th, 2016	High Resolution QL1 LiDAR

Project Site	Total Acres	Acquisition Dates	Data Type
Western Washington 3DEP – South AOI	1,617,379	March 17th, 2016 – June 6th, 2017	High Resolution QL1 LiDAR

Deliverable Products

Table 2: Products delivered to USGS for the Western Washington 3DEP sites

Western Washington 3DEP LiDAR Products Projection: Washington State Plane South Horizontal Datum: NAD83 (CORS96), Labeled HARN* Vertical Datum: NAVD88 (GEOID03) Units: US Survey Feet	
Points	LAS v 1.4 • All Classified Returns • Raw Unclassified Flightline Swaths
Rasters	3 Foot ESRI Grids • Hydroflattened Bare Earth Digital Elevation Model (DEM) • Highest Hit Digital Surface Model (DSM) 3.0 Foot GeoTiffs • Intensity Images
Vectors	Index Shapefiles (*.shp) • Site Boundary • LAS Tile Index (1/100th USGS Quadrangles) • DEM Tile Index (1/4 USGS Quadrangles) • Breaklines • Flightline Trajectories • Snow Classification Polygon Ground Survey Shapefiles (*.shp) • Non-Vegetated Ground Check Points • Vegetated Ground Check Points • Ground Control Points • Ground Control Monuments & CORS Stations

**The data were created in NAD83 (CORS96), but for GIS purposes are defined as NAD83 (HARN) as per WADNR specifications.*

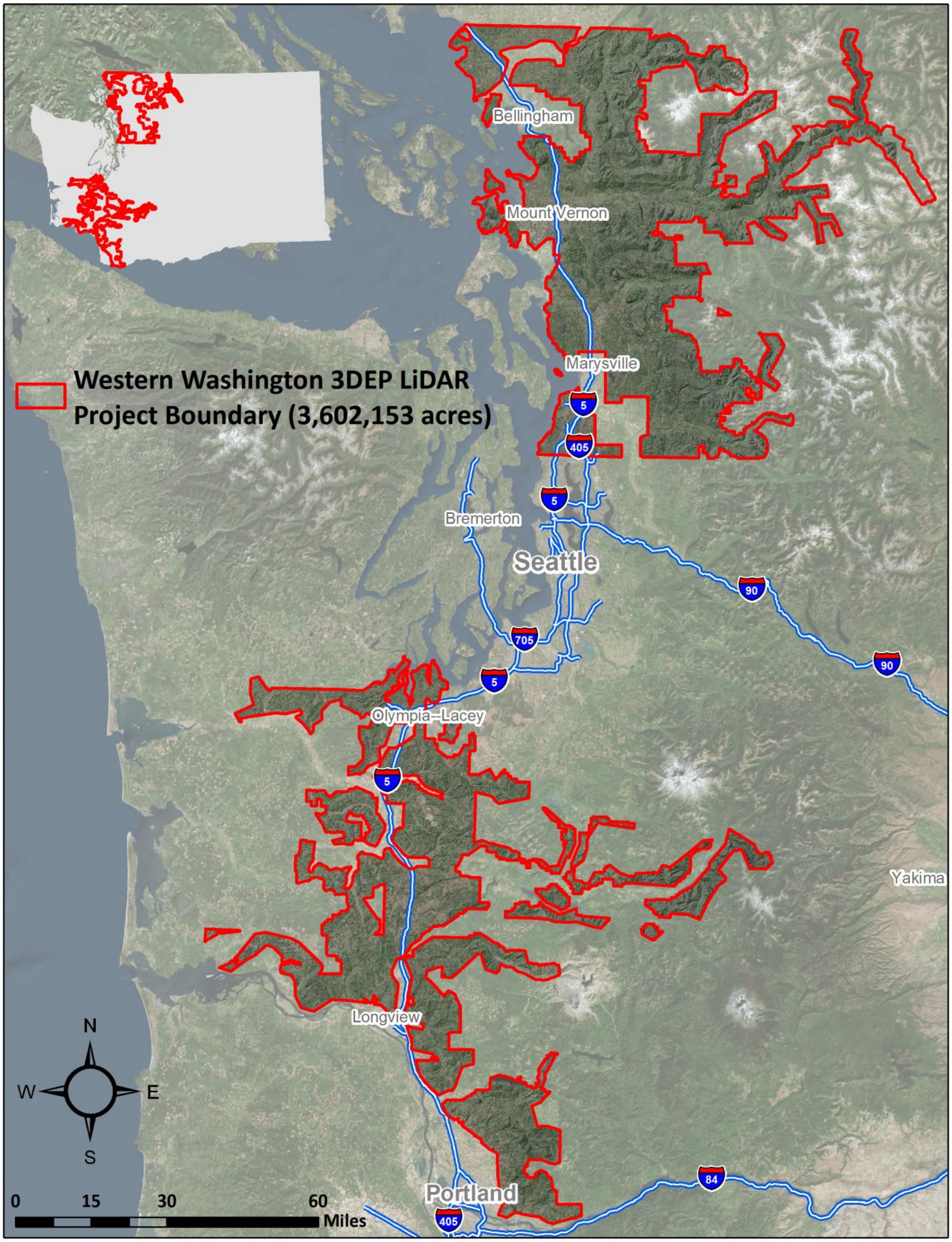

Figure 1: Location map of the Western Washington 3DEP site in Washington

ACQUISITION

QSI's static GNSS equipment set up on site in the Western Washington project area.

Planning

In preparation for data collection, QSI reviewed the project area and developed four specialized flight plans to ensure complete coverage of the Western Washington 3DEP LiDAR study area at the target point density of ≥8.0 points/m^2 (0.74 points/ft^2), to accommodate several different types of terrain within the project area. Acquisition parameters including orientation relative to terrain, flight altitude, pulse rate, scan angle, and ground speed were adapted to optimize flight paths and flight times while meeting all contract specifications.

In order to complete the acquisition and processing on an accelerated as possible timeframe, QSI subcontracted Airborne Imaging, Inc. of Alberta, Canada, and Eagle Mapping of British Columbia, Canada to acquire portions of the project area (Figure 2). Factors such as satellite constellation availability and weather windows must be considered during the planning stage. Any weather hazards or conditions affecting the flights were continuously monitored due to their potential impact on the daily success of airborne and ground operations. In addition, logistical considerations including private property access and potential air space restrictions were reviewed.

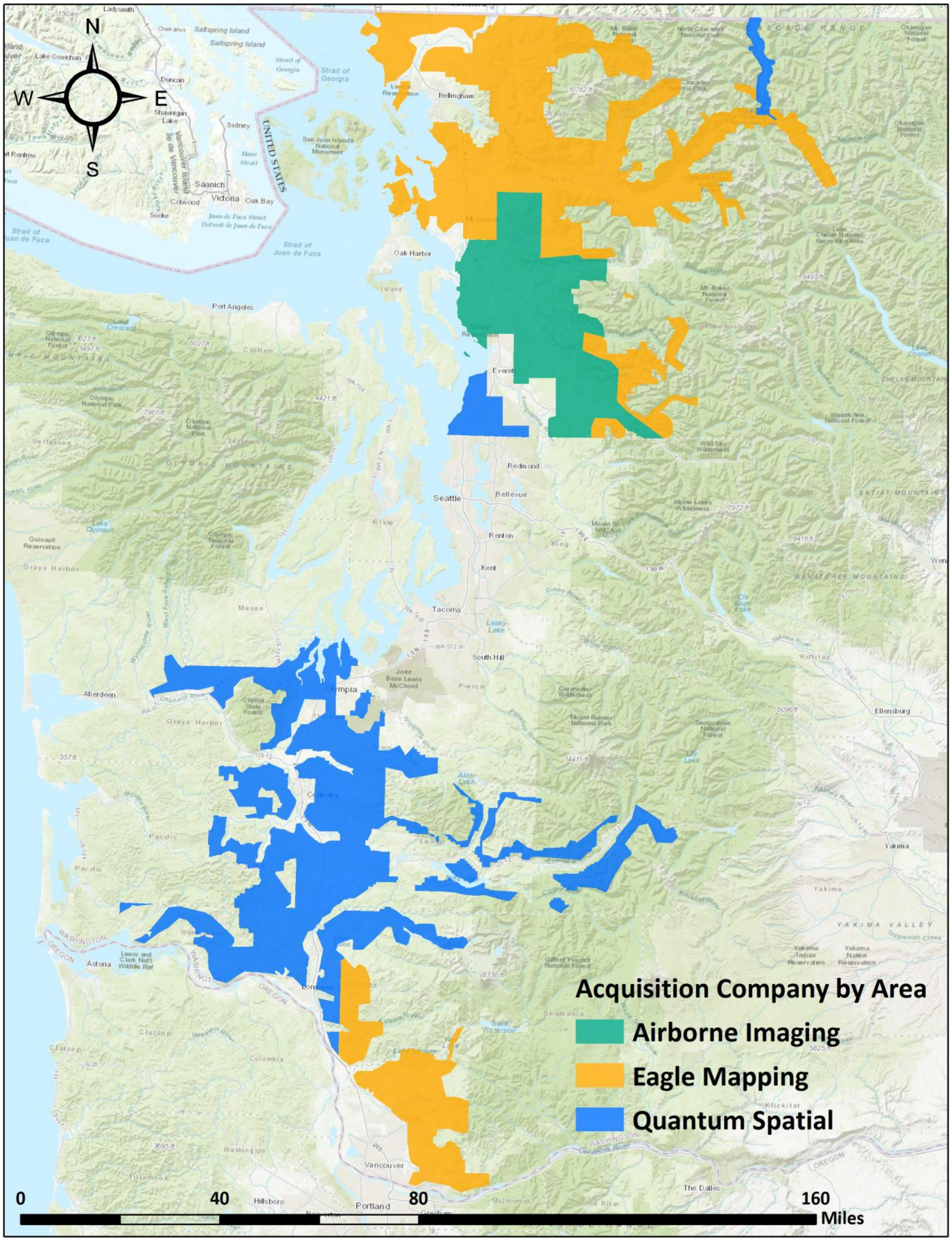

Figure 2: Western Washington Acquisition Map

Airborne LiDAR Survey

The LiDAR surveys were accomplished using Leica ALS80 sensor systems mounted in two of QSI's Cessna 208B aircrafts, in addition to Riegl Q1560 sensor systems mounted in Piper Navajo aircrafts owned by Aerial Imaging and Eagle Mapping. Table 3 summarizes the various settings used by QSI to yield an average pulse density of ≥8 pulses/m^2 over the Western Washington 3DEP project area. The Leica laser systems can record unlimited range measurements (returns) per pulse. It is not uncommon for some types of surfaces (e.g., dense vegetation or water) to return fewer pulses to the LiDAR sensor than the laser originally emitted. The discrepancy between first return and overall delivered density will vary depending on terrain, land cover, and the prevalence of water bodies. All discernible laser returns were processed for the output dataset.

All areas were surveyed with an opposing flight line side-lap of ≥50% (≥100% overlap) in order to reduce laser shadowing and increase surface laser painting. To accurately solve for laser point position (geographic coordinates x, y and z), the positional coordinates of the airborne sensor and the attitude of the aircraft were recorded continuously throughout the LiDAR data collection mission. Position of the aircraft was measured twice per second (2 Hz) by an onboard differential GPS unit, and aircraft attitude was measured 200 times per second (200 Hz) as pitch, roll and yaw (heading) from an onboard inertial measurement unit (IMU). To allow for post-processing correction and calibration, aircraft and sensor position and attitude data are indexed by GPS time.

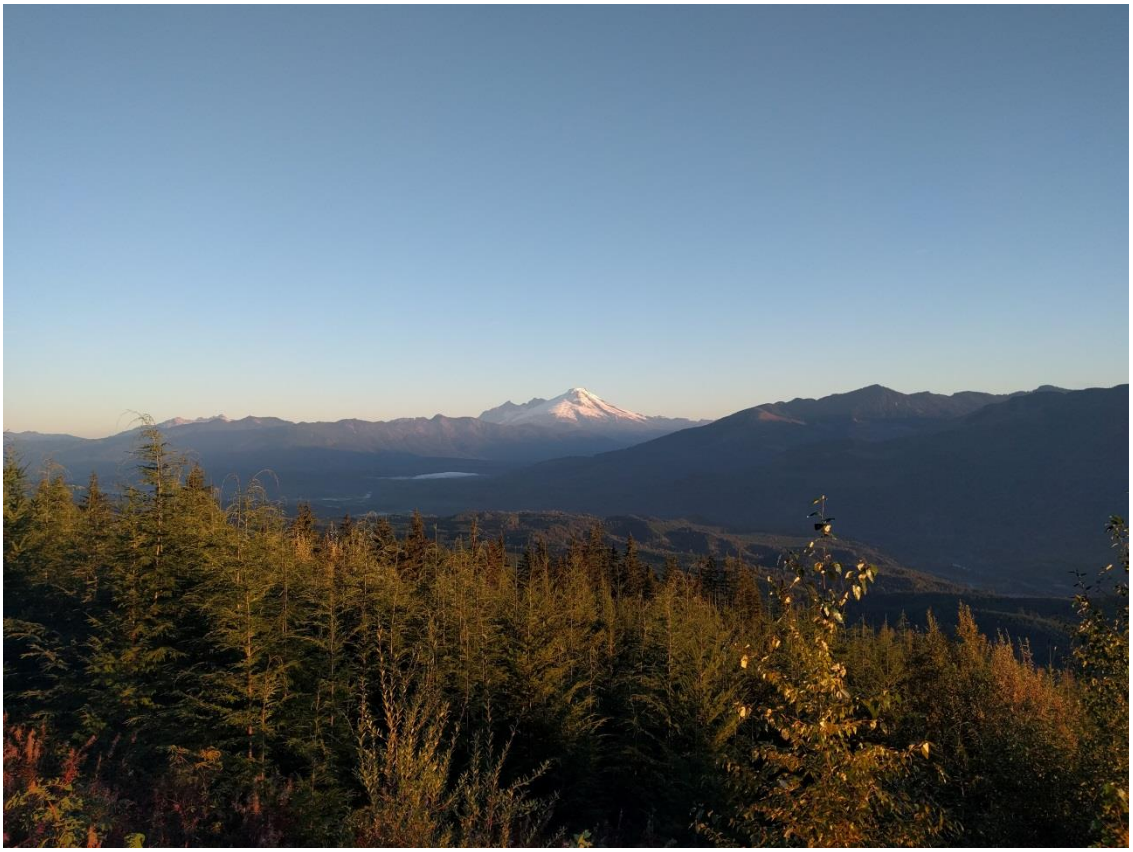

Scenic photo of the Western Washington project area taken by QSI acquisition staff

Table 3: LiDAR Flightplan Specifications

LiDAR Survey Settings & Specifications			
Operating Company	**Quantum Spatial**	**Eagle Mapping**	**Airborne Imaging**
Acquisition Dates	3/17/16 – 3/19/16, 3/26/16, 3/29/16 –4/3/16, 4/8/16 – 4/10/16, 5/7/16, 7/1/16, 7/2/16, 7/24/16, 7/25/16, 7/29/16, 7/30/16, 8/1/16, 8/3/16 – 8/6/16, 8/12/16 – 8/18/16, 12/17/16, 12/18/16, 1/23/17, 1/24/17, 1/27/17 – 1/29/17, 4/4/17, 4/11/17, 4/16/17, 5/8/17 – 5/10/17, 5/21/17, 6/6/17	3/17/16 – 3/19/16, 3/26/16, 3/29/16 – 3/30/16, 8/19/16 – 8/21/16, 8/24/16, 8/25/16, 9/13/16 – 9/15/16, 9/26/16, 9/28/16, 9/30/16, 11/03/16, 4/3/17, 4/4/17, 4/16/17, 4/17/17, 4/21/17	3/17/16, 3/18/16, 3/29/16 – 4/1/16
Aircraft Used	Cessna 208B	Piper Navajo	Piper Navajo
Sensor	Leica	Riegl	Riegl
Laser	ALS80	LMS-Q1560	LMS-Q1560
Maximum Returns	Unlimited	Unlimited	Unlimited
Resolution/Density	Average 8 pulses/m^2	Average 8 pulses/m^2	Average 8 pulses/m^2
Nominal Pulse Spacing	0.35 m	0.35 m	0.35 m
Survey Altitude (AGL)	1600 - 1700 m	1350 – 1600 m	1100 – 1900 m
Survey speed	120-140 kts	140 - 150 kts	160 kts
Field of View	30 - 40^o	60^o	60^o
Mirror Scan Rate	42 – 58.4 Hz	251 Hz	98 - 187 Hz
Target Pulse Rate	300 - 335 kHz	533.3 kHz	400 - 800 kHz
Pulse Length	2.5 ns	3 ns	3 ns
Laser Pulse Footprint Diameter	35.2 – 37.4 cm	33.8 - 40 cm	27.5 – 47.5 cm
Central Wavelength	1064 nm	1064 nm	1064 nm
Pulse Mode	Single Pulse in Air (SPiA)	Multi Pulse in Air (MPiA)	Multi Pulse in Air (MPiA)
Beam Divergence	22 mrad	25 mrad	25 mrad
Swath Width	1165 – 1240 m	1560 - 1900 m	1270 – 2200 m
Swath Overlap	60%	60%	60%
GPS Baselines	≤13 nm	≤13 nm	≤13 nm
GPS PDOP	≤3.0	≤3.0	≤3.0
GPS Satellite Constellation	≥6	≥6	≥6
Intensity	8-bit, scaled to 16-bit	8-bit, scaled to 16-bit	8-bit, scaled to 16-bit

Ground Control

Ground control surveys, including monumentation and ground survey points (GSPs) were conducted to support the airborne acquisition. Ground control data were used to geospatially correct the aircraft positional coordinate data and to perform quality assurance checks on the final LiDAR dataset.

Monuments & CORS

The spatial configuration of ground survey monuments and CORS stations provided redundant control within 13 nautical miles of the mission areas for LiDAR flights. Monuments were also used for collection of ground survey points using real time kinematic (RTK), post processed kinematic (PPK), and fast static (FS) survey techniques. Monument and CORS locations were selected with consideration for satellite visibility, field crew safety, and optimal location for GSP coverage.

QSI utilized 9 existing NGS monuments, 33 existing non-NGS monuments, and established 64 new monuments for the Western Washington 3DEP LiDAR project (Table 4, Figure 3). New monumentation was set using 5/8” x 30” rebar topped with stamped 2 ½ " aluminum caps. QSI’s professional land surveyor, Evon Silvia (WAPLS#53957) oversaw and certified the establishment of all monuments.

In addition, QSI utilized permanent static GNSS stations from three different networks as base stations for kinematic processing and GSP collection: 11 stations from the Washington State Reference Network (WSRN), 1 station from the Trimble VRS-Now network, and 2 stations from the UNAVCO Plate Boundary Observatory (PBO). See Table 6 for a full listing of CORS.

Table 4: Monuments used for the Western Washington 3DEP acquisition. Coordinates are on the NAD83 (CORS96) datum, epoch 2002.00

Monument ID	Latitude	Longitude	Ellipsoid (meters)	Containing AOI
1001_49	46° 09' 55.00263"	-123° 08' 46.34650"	-15.226	South
CH_03	46° 38' 03.90579"	-123° 15' 48.42620"	72.220	South
CH_06	46° 34' 34.04193"	-122° 50' 44.63885"	81.734	South
GCP03	46° 35' 38.67888"	-121° 49' 03.70088"	1264.885	South
MET_18	45° 33' 50.43154"	-122° 13' 20.02243"	159.902	South
OLY_03	47° 02' 50.51792"	-122° 56' 27.68599"	28.494	South
PORT_BLK_01	46° 29' 55.89039"	-122° 10' 45.38059"	219.813	South
RD4355	46° 56' 16.41534"	-122° 33' 15.51396"	78.749	South
SB0823	46° 34' 52.15463"	-121° 41' 15.59451"	291.537	South
SC2802	46° 16' 59.80355"	-122° 55' 07.79421"	-4.885	South
SC2804	46° 31' 57.86526"	-122° 43' 12.21750"	135.283	South
SC2823	46° 18' 29.49654"	-122° 17' 15.05569"	939.259	South
SC2867	46° 58' 32.98438"	-122° 53' 48.53144"	37.636	South
STA_132_E	46° 44' 40.30123"	-123° 09' 57.33921"	35.153	South
SWEWA_01	47° 04' 09.98855"	-123° 29' 33.04340"	6.701	South
SWEWA_02	46° 53' 36.63448"	-122° 51' 41.80214"	53.842	South
SWEWA_03	46° 40' 05.64189"	-123° 08' 42.14118"	55.006	South
SWEWA_04	46° 44' 01.01666"	-123° 00' 15.82667"	30.184	South
SWEWA_05	46° 45' 38.69743"	-122° 49' 08.76104"	44.686	South

Monument ID	Latitude	Longitude	Ellipsoid (meters)	Containing AOI
SWEWA_06	46° 39' 59.14330"	-122° 46' 16.49931"	105.237	South
SWEWA_07	46° 51' 28.04466"	-122° 40' 09.26881"	115.458	South
SWEWA_08	46° 37' 07.46875"	-122° 28' 55.65974"	648.029	South
SWEWA_09	46° 36' 47.85239"	-122° 25' 39.80548"	909.871	South
SWEWA_10	46° 32' 42.54170"	-121° 59' 21.80296"	462.345	South
SWEWA_11	46° 37' 25.78171"	-121° 41' 04.06678"	319.861	South
SWEWA_12_RTK	46° 38' 16.15917"	-121° 23' 31.12318"	1343.120	South
SWEWA_13	46° 41' 07.24020"	-122° 11' 45.80503"	473.568	South
SWEWA_14	46° 39' 48.36726"	-122° 11' 57.75518"	506.212	South
SWEWA_15	46° 29' 17.37334"	-121° 48' 27.05303"	1124.232	South
SWEWA_16	46° 18' 41.04587"	-122° 22' 28.34284"	877.072	South
SWEWA_17	46° 29' 58.90485"	-122° 22' 12.97495"	398.922	South
SWEWA_18	45° 45' 34.80966"	-122° 19' 26.13912"	340.625	South
SWEWA_19	45° 41' 52.17668"	-122° 20' 39.58449"	485.974	South
SWEWA_20	46° 16' 18.91473"	-122° 56' 15.89041"	-5.791	South
SWEWA_21	46° 16' 18.78672"	-122° 56' 24.63121"	-5.510	South
SWEWA_22	46° 31' 04.75315"	-122° 52' 26.62970"	124.839	South
SWEWA_23	45° 39' 00.03099"	-122° 24' 50.20599"	97.188	South
SWEWA_24	46° 26' 56.75768"	-122° 51' 20.48429"	71.132	South
SWEWA_25	46° 23' 22.11629"	-122° 53' 58.19844"	31.641	South
SWEWA_26	46° 33' 40.41661"	-123° 07' 47.13463"	55.008	South
SWEWA_27	46° 23' 09.78834"	-123° 05' 37.42758"	162.619	South
SWEWA_28	46° 11' 57.93209"	-123° 10' 03.73341"	89.901	South
SWEWA_29	46° 16' 09.22173"	-123° 27' 40.38819"	-15.451	South
SWEWA_30	45° 53' 36.59403"	-122° 33' 03.04586"	226.255	South
SWEWA_31	46° 19' 40.51477"	-122° 29' 18.25954"	414.677	South
SWEWA_RTK_01	46° 33' 11.26120"	-123° 19' 12.42597"	118.594	South
SY1376	47° 00' 31.65341"	-123° 22' 32.34274"	-3.906	South
SY1395	47° 01' 58.83498"	-123° 06' 44.64190"	132.558	South
WA_DNR_P2_04	46° 03' 45.14132"	-122° 45' 18.81570"	321.507	South
WASCO_50	46° 31' 29.10560"	-121° 57' 18.86287"	251.406	South
WSDOT_5519	46° 47' 25.01657"	-122° 44' 13.89361"	82.378	South
WSDOT_CONTROL_01	46° 06' 26.66566"	-122° 53' 06.72502"	-13.587	South
BM31530	48° 16' 20.02030"	-121° 54' 02.74797"	53.464	North
CEDAR_9	47° 48' 30.30271"	-121° 59' 57.61062"	-11.421	North
DH3744	48° 43' 02.85680"	-122° 30' 41.96336"	-4.197	North
GP31531	48° 09' 07.86696"	-122° 09' 05.51826"	16.093	North
MTBAKER_04	48° 48' 13.32476"	-121° 54' 07.90910"	1198.377	North
NF_NOOK_01	48° 53' 34.32924"	-121° 57' 54.54739"	248.930	North
NOOK_10	48° 50' 26.36404"	-122° 08' 55.21014"	72.151	North
NOOK_12_RES	48° 41' 08.70501"	-122° 11' 29.81218"	76.407	North
NWEWA_01	48° 00' 54.88242"	-122° 06' 00.73932"	46.643	North
NWEWA_02	48° 30' 56.06205"	-122° 24' 40.24011"	-16.620	North
NWEWA_03	47° 58' 41.97698"	-122° 03' 14.78868"	9.736	North

Monument ID	Latitude	Longitude	Ellipsoid (meters)	Containing AOI
NWEWA_04	48° 53' 16.19629"	-122° 32' 24.92054"	-2.070	North
NWEWA_05	48° 19' 36.21590"	-122° 08' 54.20088"	144.900	North
NWEWA_06	48° 31' 23.37842"	-122° 11' 40.22041"	0.279	North
NWEWA_07	48° 18' 29.25137"	-122° 17' 07.60153"	79.231	North
NWEWA_08	48° 53' 01.03521"	-122° 18' 34.88113"	15.853	North
NWEWA_09	48° 43' 09.36882"	-121° 07' 16.32320"	351.629	North
NWEWA_10	48° 50' 46.15207"	-121° 41' 33.49037"	1534.125	North
NWEWA_11	48° 55' 27.23482"	-122° 04' 40.71479"	177.816	North
NWEWA_12	48° 49' 19.38786"	-121° 56' 32.63326"	1400.660	North
NWEWA_13	48° 41' 22.96410"	-121° 37' 59.58869"	1151.236	North
NWEWA_14	48° 41' 23.00965"	-121° 37' 59.32551"	1150.433	North
NWEWA_15	48° 31' 35.57415"	-121° 25' 35.12804"	77.597	North
NWEWA_16	48° 30' 23.39465"	-121° 16' 43.79068"	963.083	North
NWEWA_17	48° 41' 08.13930"	-120° 53' 06.86861"	673.077	North
NWEWA_18	48° 38' 38.11855"	-120° 51' 15.79268"	932.517	North
NWEWA_20	48° 25' 51.12877"	-121° 54' 23.88386"	796.468	North
NWEWA_21	48° 26' 15.85480"	-121° 56' 05.63655"	900.544	North
NWEWA_22	48° 29' 40.87081"	-121° 32' 27.28706"	58.701	North
NWEWA_23	48° 27' 15.37739"	-121° 39' 53.51859"	693.646	North
NWEWA_24	48° 28' 00.38075"	-121° 40' 25.80714"	339.481	North
NWEWA_25	47° 49' 13.64344"	-121° 33' 23.14817"	144.797	North
NWEWA_27	48° 06' 18.73743"	-121° 50' 02.24804"	258.002	North
NWEWA_28	48° 04' 13.17699"	-121° 38' 44.88542"	375.953	North
NWEWA_29	48° 02' 26.85449"	-121° 38' 27.92150"	889.275	North
NWEWA_30	48° 28' 37.29086"	-122° 09' 26.53658"	137.893	North
NWEWA_31	48° 20' 36.23589"	-122° 02' 04.84998"	363.836	North
NWEWA_32	48° 02' 48.48978"	-121° 42' 37.86144"	743.225	North
OM2	48° 12' 42.89508"	-122° 20' 20.81348"	-18.016	North
PSLC_KNG_01	47° 46' 22.86514"	-121° 29' 09.79972"	212.816	North
PSLC_KNG_15	47° 24' 24.79988"	-122° 19' 21.88588"	21.086	North
PSLC_KNG_16	47° 50' 20.37391"	-122° 12' 54.69201"	60.916	North
SPIKE_01	48° 50' 51.53178"	-121° 41' 27.73734"	1513.000	North
TULA_05	47° 52' 17.73585"	-121° 46' 23.51549"	41.374	North
TULA_3	48° 12' 46.16465"	-122° 02' 55.75517"	76.522	North
VISTA_1973	48° 42' 35.11158"	-121° 05' 50.36617"	498.993	North
WA_EST_06	48° 27' 13.24735"	-122° 31' 02.40344"	-13.373	North
WHAT_03	48° 37' 49.46041"	-122° 18' 58.96557"	104.297	North
WSDOT_1638	48° 16' 09.07106"	-121° 40' 53.17468"	120.597	North
WSDOT_1935	48° 21' 44.46493"	-122° 12' 19.56849"	12.416	North
WSDOT_3283	48° 32' 14.44786"	-121° 46' 11.01931"	36.298	North
WSDOT_4048	48° 04' 59.85591"	-121° 58' 34.24260"	99.510	North

To correct the continuously recorded onboard measurements of the aircraft position, QSI concurrently conducted multiple static Global Navigation Satellite System (GNSS) ground surveys (1 Hz recording frequency) over each monument. During post-processing, the static GPS data were triangulated with nearby Continuously Operating Reference Stations (CORS) using the Online Positioning User Service (OPUS[1]) for precise positioning. Multiple independent sessions over the same monument were processed to confirm antenna height measurements and to refine position accuracy.

Monuments were established according to the national standard for geodetic control networks, as specified in the Federal Geographic Data Committee (FGDC) Geospatial Positioning Accuracy Standards for geodetic networks.[2] This standard provides guidelines for classification of monument quality at the 95% confidence interval as a basis for comparing the quality of one control network to another. The monument rating for this project is shown in Table 5.

Table 5: Federal Geographic Data Committee monument rating for network accuracy

Direction	Rating
1.96 * St Dev $_{NE}$:	0.050 m
1.96 * St Dev $_{z}$:	0.050 m

For the Western Washington 3DEP LiDAR project, the monument coordinates contributed no more than the listed positional error to the geolocation of the final ground survey points and LiDAR, with 95% confidence.

Table 6: CORS used for the Western Washington 3DEP acquisition. Coordinates are on the NAD83 (CORS96) datum, epoch 2002.00

CORS ID	Owner	Latitude	Longitude	Ellipsoid (meters)	Containing AOI
CATH	WSRN	46° 11' 50.27352"	-123° 22' 02.11585"	56.680	South
COUG	WSRN	46° 03' 33.16130"	-122° 15' 38.72844"	151.845	South
CPXF	WSRN	46° 50' 24.29003"	-122° 15' 23.40937"	534.002	South
CROK	WSRN	46° 16' 28.54263"	-122° 54' 45.09639"	1.482	South
GRMD	WSRN	46° 47' 43.73313"	-123° 01' 21.29229"	31.067	South
P397	PBO	46° 25' 17.81194"	-123° 47' 56.92030"	566.638	South
PKWD	WSRN	46° 35' 59.25492"	-121° 40' 37.07190"	307.098	South
TPW2	PBO	46° 12' 26.52494"	-123° 46' 06.05131"	-14.606	South
VCWA	WSRN	45° 37' 03.44172"	-122° 30' 57.80035"	77.415	South
WAWA	WSRN	45° 35' 16.90033"	-122° 21' 08.39388"	6.866	South
WEBG	VRS Now	45° 46' 46.45966"	-122° 33' 46.11748"	67.674	South
LSIG	WSRN	47° 41' 42.70671"	-121° 41' 22.37407"	527.517	North
P444	WSRN	48° 43' 48.77186"	-121° 04' 03.11143"	494.233	North
VERN	WSRN	48° 25' 04.25592"	-122° 20' 13.86999"	5.654	North

[1] OPUS is a free service provided by the National Geodetic Survey to process corrected monument positions. http://www.ngs.noaa.gov/OPUS.

[2] Federal Geographic Data Committee, Geospatial Positioning Accuracy Standards (FGDC-STD-007.2-1998). Part 2: Standards for Geodetic Networks, Table 2.1, page 2-3. http://www.fgdc.gov/standards/projects/FGDC-standards-projects/accuracy/part2/chapter2

Ground Survey Points (GSPs)

Ground survey points were collected using real time kinematic (RTK), post-processed kinematic (PPK), and fast-static (FS) survey techniques. A Trimble R7, R6, or R8 base unit was positioned at a nearby monument to broadcast a kinematic correction to a roving Trimble R6, R10, or R8 GNSS receiver. All GSP measurements were made during periods with a Position Dilution of Precision (PDOP) of ≤ 3.0 with at least six satellites in view of the stationary and roving receivers. When collecting RTK and PPK data, the rover records data while stationary for five seconds, then calculates the pseudorange position using at least three one-second epochs. FS surveys record observations for up to fifteen minutes on each GSP in order to support longer baselines for post-processing. Relative errors for any GSP position must be less than 1.5 cm horizontal and 2.0 cm vertical in order to be accepted. See Table 7 for Trimble unit specifications. CORS equipment specifications are not included.

GSPs were collected in areas where good satellite visibility was achieved on paved roads and other hard surfaces such as gravel or packed dirt roads. GSP measurements were not taken on highly reflective surfaces such as center line stripes or lane markings on roads due to the increased noise seen in the laser returns over these surfaces. GSPs were collected within as many flightlines as possible; however the distribution of GSPs depended on ground access constraints and monument locations and may not be equitably distributed throughout the study area (Figure 3).

Table 7: Trimble equipment identification

Receiver Model	Antenna	OPUS Antenna ID	Use
Trimble R6	Integrated GNSS Antenna R6	TRM_R6	Static, Rover
Trimble R7 GNSS	Zephyr GNSS Geodetic Model 2 RoHS	TRM57971.00	Static, Rover
Trimble R8	Integrated Antenna R8 Model 2	TRM_R8_GNSS	Static, Rover
Trimble R10	Integrated Antenna R10	TRMR10	Rover

Land Cover Class

In addition to ground survey points, land cover class check points were collected throughout the study area to evaluate vertical accuracy. Vertical accuracy statistics were calculated for all land cover types to assess confidence in the LiDAR derived ground models across land cover classes (Table 8, see LiDAR Accuracy Assessments, page 22).

Table 8: Land Cover Types and Descriptions

Land cover type	Land cover code	Example	Description	Accuracy Assessment Type
Bare Earth	BARE, DRT, GVL, PVD		Areas of bare earth surface	NVA
Urban	URBAN, URBAN_PVD, URBAN_AREA		Areas of urban development	NVA
Tall Grass	TALL_GRASS		Herbaceous grasslands in advanced stages of growth	VVA
Shrubland	SHRUB		Herbaceous shrublands	VVA
Mixed Forest	FOREST, EVER_FOREST, DEC_FOR, MX_FOR		Forested areas comprised of both deciduous and coniferous species	VVA

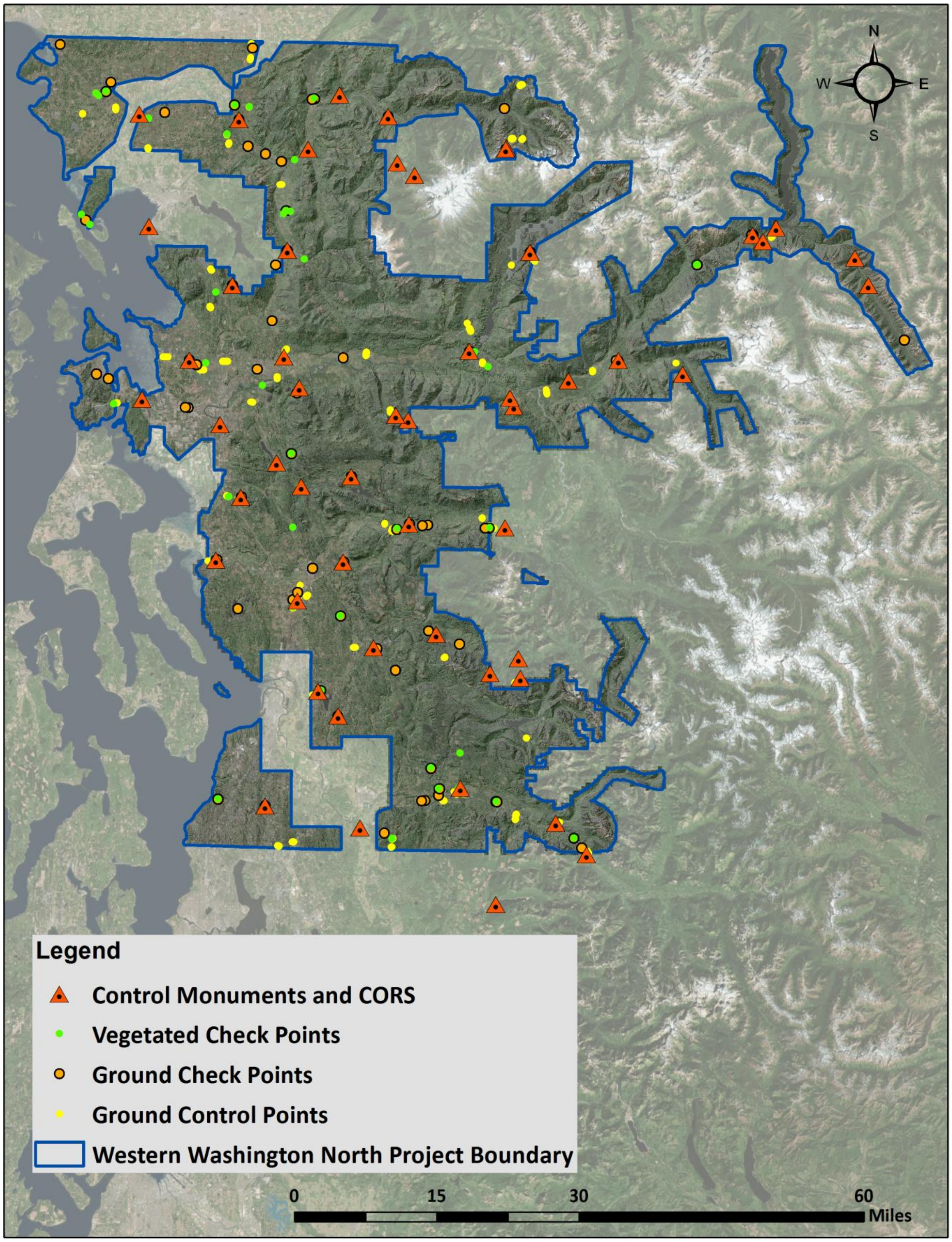

Figure 3: North AOI ground survey location map

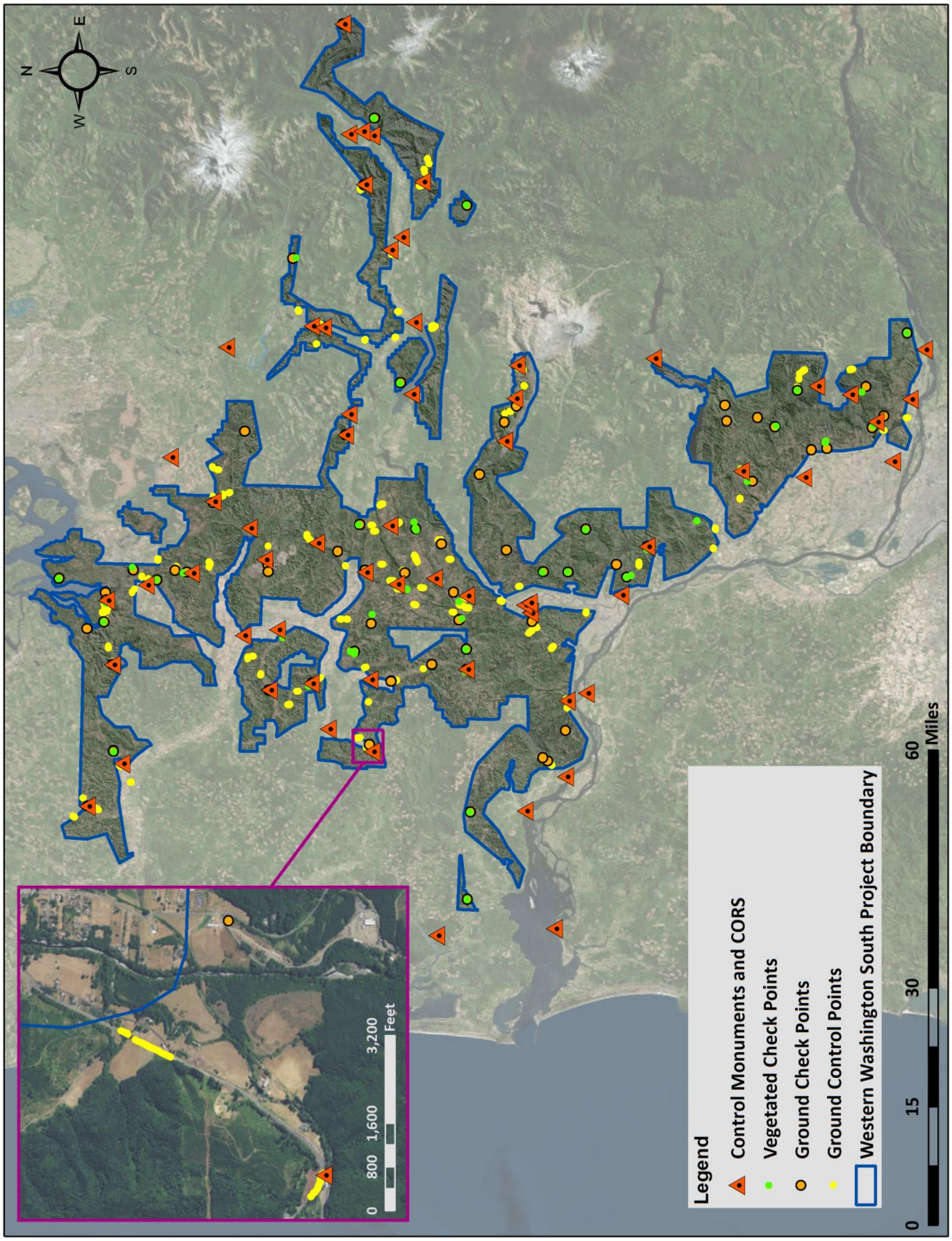

Figure 4: South AOI ground survey location map

PROCESSING

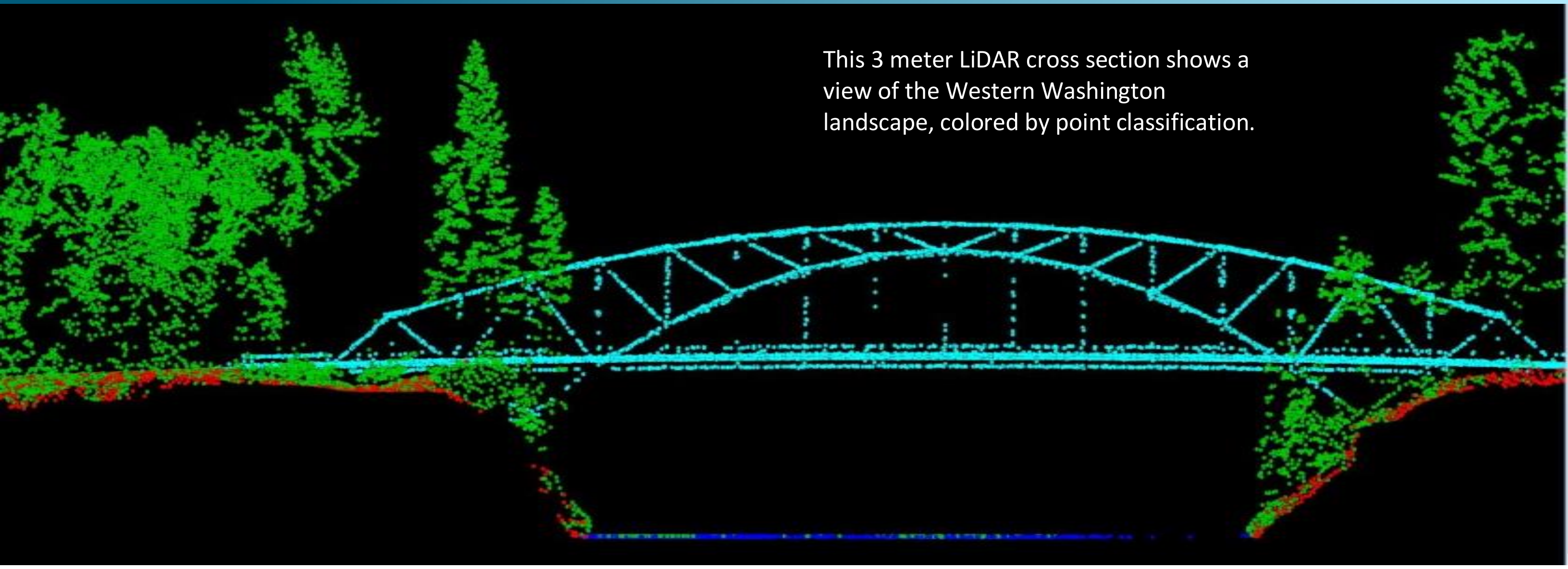

This 3 meter LiDAR cross section shows a view of the Western Washington landscape, colored by point classification.

LiDAR Data

Upon completion of data acquisition, QSI processing staff initiated a suite of automated and manual techniques to process the data into the requested deliverables. Processing tasks included GPS control computations, smoothed best estimate trajectory (SBET) calculations, kinematic corrections, calculation of laser point position, sensor and data calibration for optimal relative and absolute accuracy, and LiDAR point classification (Table 9). Processing methodologies were tailored for the landscape. Brief descriptions of these tasks are shown in Table 10.

Table 9: ASPRS LAS classification standards applied to the Western Washington 3DEP dataset

Classification Number	Classification Name	Classification Description
1	Default/Unclassified	Laser returns that are not included in the ground class, composed of vegetation and anthropogenic features
2	Ground	Laser returns that are determined to be ground using automated and manual cleaning algorithms
9	Water	Laser returns that are determined to be water using automated and manual cleaning algorithms
10	Ignored Ground	Ground points proximate to water’s edge breaklines; ignored for correct model creation
17	Bridge	Bridge decks

Classification Number	Classification Name	Classification Description
21	Temporal Snow	Areas which were observed to have possible snow coverage, identified during LiDAR acquisition
22	Temporal Ground	Areas within the project area which experienced temporal change in the ground surface due to a landslide
23	Temporal Default	Vegetation within the project area which experienced temporal change due to a landslide

Temporal Snow Classification

While collecting the Western Washington North LiDAR dataset, QSI acquisition teams made note of areas within the project site that appeared to have, or may have had, snow on the ground, which would affect the laser's ability to penetrate to the ground surface. These areas were identified by manually drawing temporal snow polygons during acquisition. Later, during LiDAR processing, specific care was taken to edit the initial snow polygons to better identify and reclassify areas that may contain snow, which could cause temporal differences in the ground surface of the LiDAR point cloud. These areas should be considered to be ground classified, with the potential use limitation taken into account for any analysis purposes (Table 9).

Temporal Ground & Default

During the timeframe of LiDAR collection for the Western Washington 3DEP project, a small landslide occurred along the Toutle River, causing significant temporal offsets in the ground surface and vegetation between flightlines in that area. In order to maintain LiDAR coverage in the area and a true representation of the most recent ground surface, QSI classified ground and default for the affected missions (flown on August 18th, 2016, and May 10th, 2017), to holding classifications 22 - temporal ground, and 23 - temporal default, respectively (Table 9).

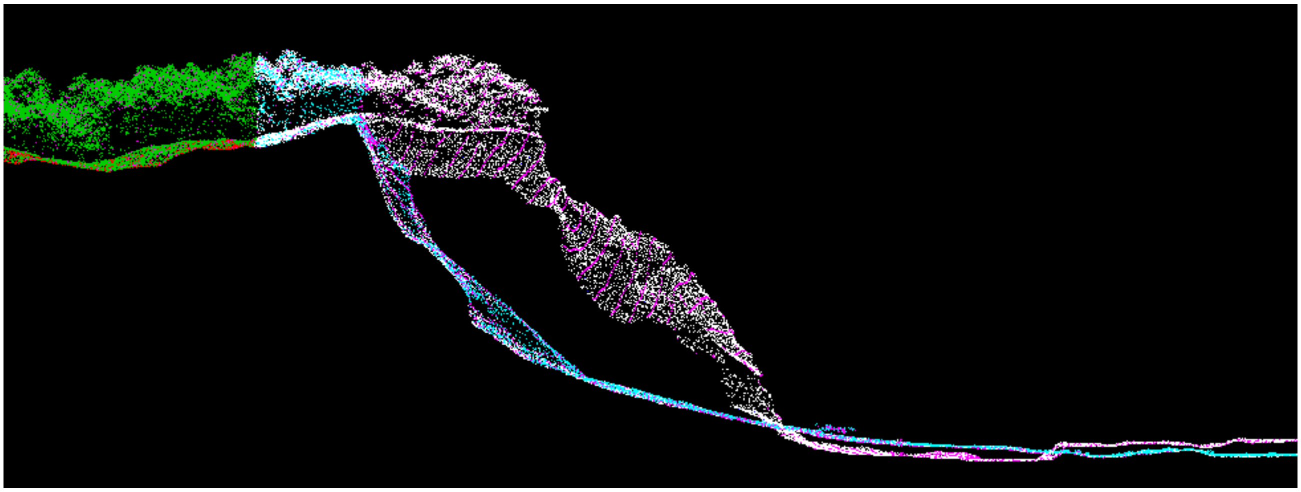

Figure 5: This LiDAR cross section shows a view of a landslide which occurred along the Toutle River, and the temporal difference between the topography captured during LiDAR acquisition

Table 10: LiDAR processing workflow

LiDAR Processing Step	Software Used
Resolve kinematic corrections for aircraft position data using kinematic aircraft GPS and static ground GPS data. Develop a smoothed best estimate of trajectory (SBET) file that blends post-processed aircraft position with sensor head position and attitude recorded throughout the survey.	Waypoint Inertial Explorer v.8.6 & v.8.7 PosPAC MMS v.7.SP3 & v.8.0
Calculate laser point position by associating SBET position to each laser point return time, scan angle, intensity, etc. Create raw laser point cloud data for the entire survey in *.las (ASPRS v. 1.4) format. Convert data to orthometric elevations by applying a geoid correction.	Waypoint Inertial Explorer v.8.6 Leica Cloudpro v. 1.2.2 & v. 1.2.4 SDCImport v.2.0.1 RiProcess v.1.8.1 RiWorld v.5.0.2
Import raw laser points into manageable blocks (less than 500 MB) to perform manual relative accuracy calibration and filter erroneous points. Classify ground points for individual flight lines.	TerraScan v.17
Using ground classified points per each flight line, test the relative accuracy. Perform automated line-to-line calibrations for system attitude parameters (pitch, roll, heading), mirror flex (scale) and GPS/IMU drift. Calculate calibrations on ground classified points from paired flight lines and apply results to all points in a flight line. Use every flight line for relative accuracy calibration.	TerraMatch v.17
Classify resulting data to ground and other client designated ASPRS classifications (Table 2). Assess statistical absolute accuracy via direct comparisons of ground classified points to ground control survey data.	Las Monkey 2.2.7 (QSI proprietary) TerraScan v.17 TerraModeler v.17
Generate bare earth models as triangulated surfaces. Generate highest hit models as a surface expression of all classified points. Export all surface models as ESRI GRIDs at a 3.0 foot pixel resolution.	TerraScan v.17 TerraModeler v.17 ArcMap v. 10.2.2
Correct intensity values for variability and export intensity images as GeoTIFFs at a 3.0 foot pixel resolution.	Las Monkey 2.2.7 (QSI proprietary) LAS Product Creator 1.5 (QSI proprietary) ArcMap v. 10.3.1

Intensity Normalization

Laser return intensity is a unitless measure of discrete return voltage, stored as an integer value from 0 to 65,535 (16-bit). Intensity values correspond to the reflectivity of the surface, which is a function of surface material composition. The magnitude of intensity values can vary across similar surfaces due to variability in receiver fixed or auto gain control (AGC), atmospherics, target range, and the angle of incidence. These components influence intensity at different rates and magnitudes, with AGC comprising the majority of influence. The result is line to line inconsistency and streaking in the images that can reduce the utility of these data for analysis.

QSI utilized proprietary software to minimize variability caused by fixed gain control, atmospheric transmissivity, range differences, and the angle of incidence to arrive at a normalized intensity value that approaches a true radiometric value for each discrete laser return.

Feature Extraction

Hydro-flattening and Water's edge breaklines

The ocean surrounding the Western Washington 3DEP site and other water bodies within the project area were flattened to a consistent water level. Bodies of water that were flattened include lakes and other closed water bodies with a surface area greater than 2 acres, all streams and rivers that are nominally wider than 100 feet, and all tidal waters bordering the project. Islands within water bodies with area greater than 1 acre were not hydroflattened, with select smaller islands and features remaining as feasible. The hydroflattening process eliminates artifacts in the digital terrain model caused by both increased variability in ranges or dropouts in laser returns due to the low reflectivity of water.

Hydroflattening of closed water bodies was performed through a combination of automated and manual detection and adjustment techniques designed to identify water boundaries and water levels. Boundary polygons were developed using an algorithm which weights LiDAR-derived slopes, intensities, and return densities to detect the water's edge. The water edges were then manually reviewed and edited as necessary.

Once polygons were developed the initial ground classified points falling within water polygons were reclassified as water points to omit them from the final ground model. Elevations were then obtained from the filtered LiDAR returns to create the final breaklines. Lakes were assigned a consistent elevation for an entire polygon while rivers were assigned consistent elevations on opposing banks and smoothed to ensure downstream flow through the entire river channel.

Water boundary breaklines were then incorporated into the hydro-flattened DEM by enforcing triangle edges (adjacent to the breakline) to the elevation values of the breakline. This implementation corrected interpolation along the hard edge. Water surfaces were obtained from a TIN of the 3-D water edge breaklines resulting in the final hydroflattened model.

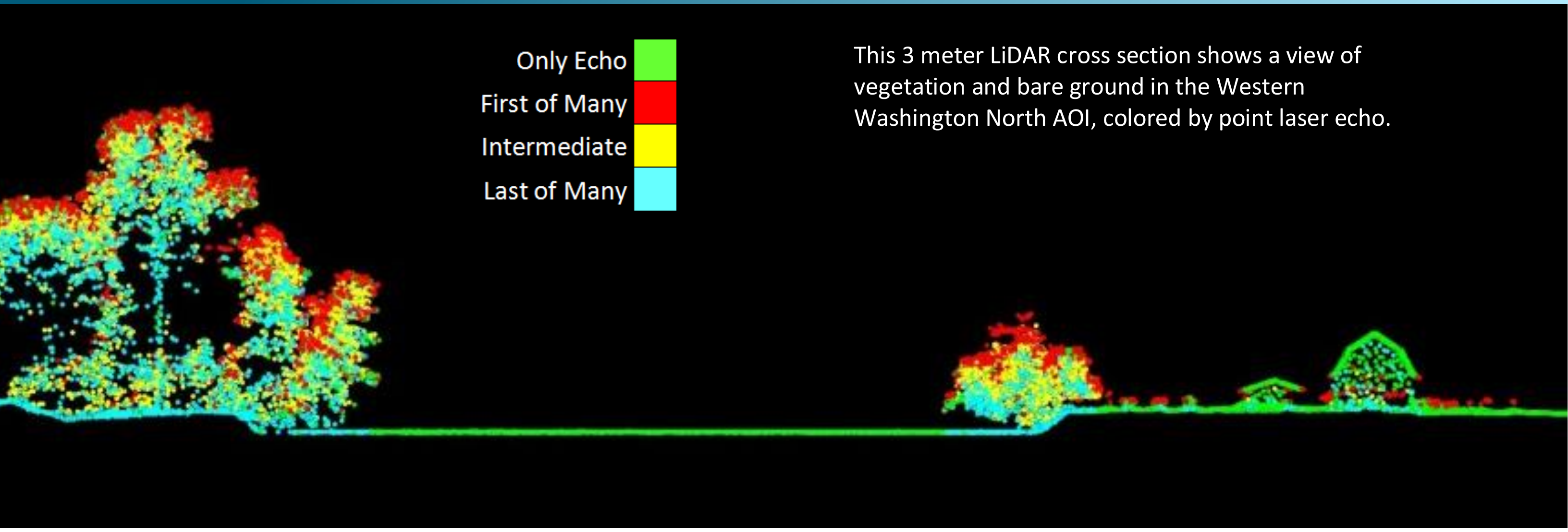

This 3 meter LiDAR cross section shows a view of vegetation and bare ground in the Western Washington North AOI, colored by point laser echo.

LiDAR Density

The acquisition parameters were designed to acquire an average first-return density of 8 points/m^2 (0.74 points/ft^2). First return density describes the density of pulses emitted from the laser that return at least one echo to the system. Multiple returns from a single pulse were not considered in first return density analysis. Some types of surfaces (e.g., breaks in terrain, water and steep slopes) may have returned fewer pulses than originally emitted by the laser. First returns typically reflect off the highest feature on the landscape within the footprint of the pulse. In forested or urban areas the highest feature could be a tree, building or power line, while in areas of unobstructed ground, the first return will be the only echo and represents the bare earth surface.

The density of ground-classified LiDAR returns was also analyzed for this project. Terrain character, land cover, and ground surface reflectivity all influenced the density of ground surface returns. In vegetated areas, fewer pulses may penetrate the canopy, resulting in lower ground density.

The average first-return density of LiDAR data for the Western Washington 3DEP project was 1.14 points/ft^2 (12.29 points/m^2) while the average ground classified density was 0.23 points/ft^2 (2.46 points/m^2) (Table 11). The statistical distribution of first return densities and classified ground return densities per 300 ft x 300 ft cell are portrayed in Figure 6 and Figure 7, respectively.

Table 11: Average LiDAR point densities

Classification	Point Density
First-Return	1.14 points/ft^2 12.29 points/m^2
Ground Classified	0.23 points/ft^2 2.46 points/m^2

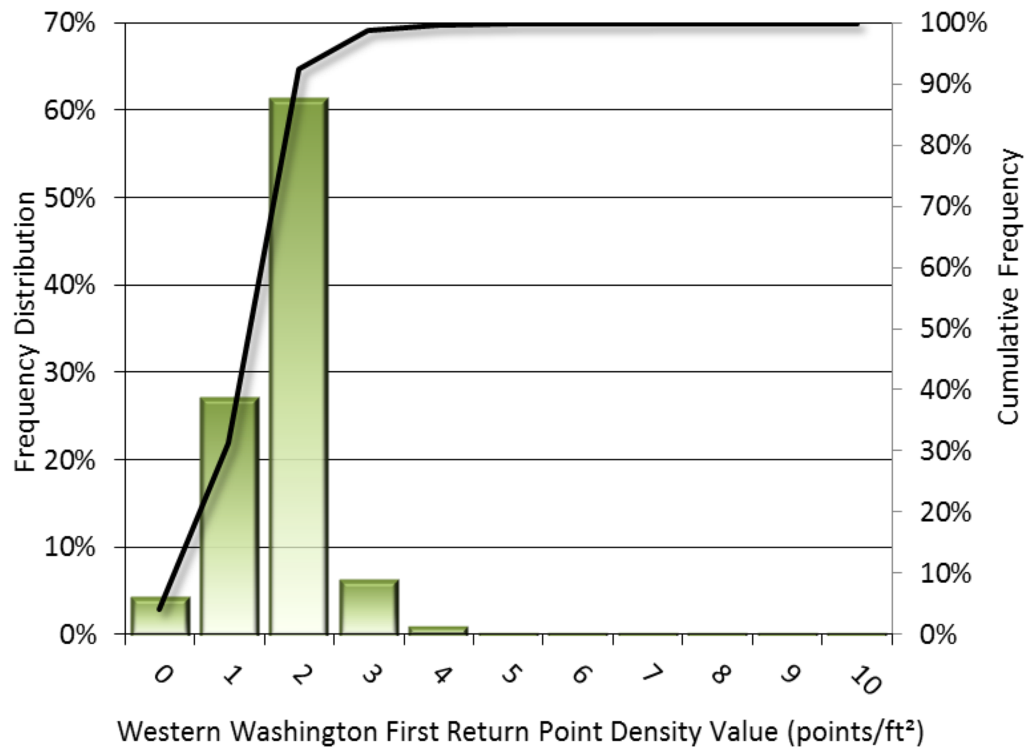

Figure 6: Frequency distribution of first return point density values per 300 x 300 ft cell

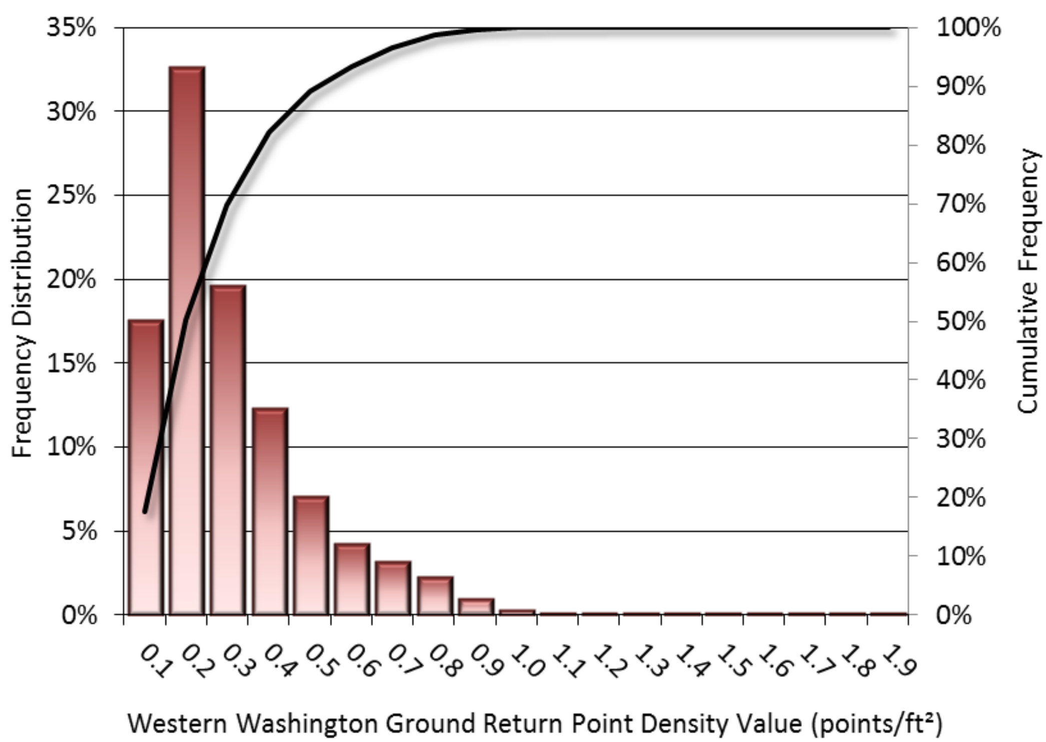

Figure 7: Frequency distribution of ground-classified return point density values per 300 x 300 ft cell

LiDAR Accuracy Assessments

The accuracy of the LiDAR data collection can be described in terms of absolute accuracy (the consistency of the data with external data sources) and relative accuracy (the consistency of the dataset with itself). See Appendix A for further information on sources of error and operational measures used to improve relative accuracy.

LiDAR Non-vegetated Vertical Accuracy

Absolute vertical accuracy was assessed using Non-Vegetated Vertical Accuracy (NVA) reporting designed to meet guidelines presented in the FGDC National Standard for Spatial Data Accuracy[3] (NSSDA). NVA compares known ground quality assurance point data collected on open, bare earth surfaces with level slope (<20°) to the triangulated surface generated by the LiDAR points. NVA is a measure of the accuracy of LiDAR point data in open areas where the LiDAR system has a high probability of measuring the ground surface and is evaluated at the 95% confidence interval (1.96 * RMSE), as shown in Table 12.

The mean and standard deviation (sigma σ) of divergence of the ground surface model from quality assurance point coordinates are also considered during accuracy assessment. These statistics assume the error for x, y and z is normally distributed, and therefore the skew and kurtosis of distributions are also considered when evaluating error statistics. For the Western Washington 3DEP survey, 182 quality assurance points tested 0.267 feet (0.081 meters) vertical accuracy at 95 percent confidence level as compared to the bare earth DEM (Figure 8). As compared to the unclassified point cloud, 182 quality assurance points tested 0.263 feet (0.080 meters) vertical accuracy at 95 percent confidence level (Figure 9).

QSI also assessed absolute accuracy using 14,675 supplemental ground control points. Although these points were used in the calibration and post-processing of the LiDAR point cloud, they still provide a good indication of the overall accuracy of the LiDAR dataset, and therefore have been provided in Table 12 and Figure 10.

---

[3] Federal Geographic Data Committee, ASPRS POSITIONAL ACCURACY STANDARDS FOR DIGITAL GEOSPATIAL DATA EDITION 1, Version 1.0, NOVEMBER 2014. http://www.asprs.org/PAD-Division/ASPRS-POSITIONAL-ACCURACY-STANDARDS-FOR-DIGITAL-GEOSPATIAL-DATA.html.

Table 12: Absolute accuracy results

Absolute Accuracy			
	Quality Assurance Points (NVA), as compared to Bare Earth DEM	Quality Assurance Points (NVA), as compared to unclassified LAS	Supplemental Ground Control Points
Sample	182 points	182 points	14,675 points
NVA (1.96*RMSE)	0.267 ft 0.081 m	0.263 ft 0.080 m	0.204 ft 0.062 m
Average	-0.011 ft -0.003 m	0.047 ft 0.014 m	-0.029 ft -0.009 m
Median	-0.026 ft -0.008 m	0.036 ft 0.011 m	-0.030 ft -0.009 m
RMSE	0.136 ft 0.042 m	0.134 ft 0.041 m	0.104 ft 0.032 m
Standard Deviation (1σ)	0.136 ft 0.042 m	0.126 ft 0.038 m	0.100 ft 0.030 m

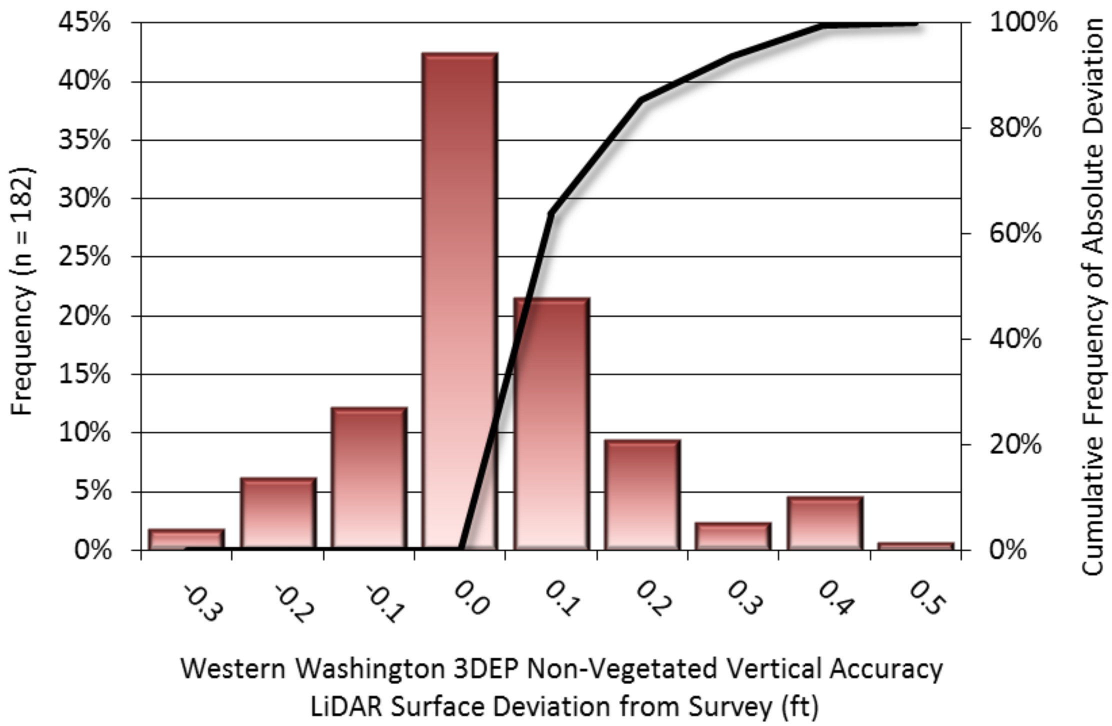

Figure 8: Frequency histogram for LiDAR DEM surface deviation from non-vegetated quality assurance point values

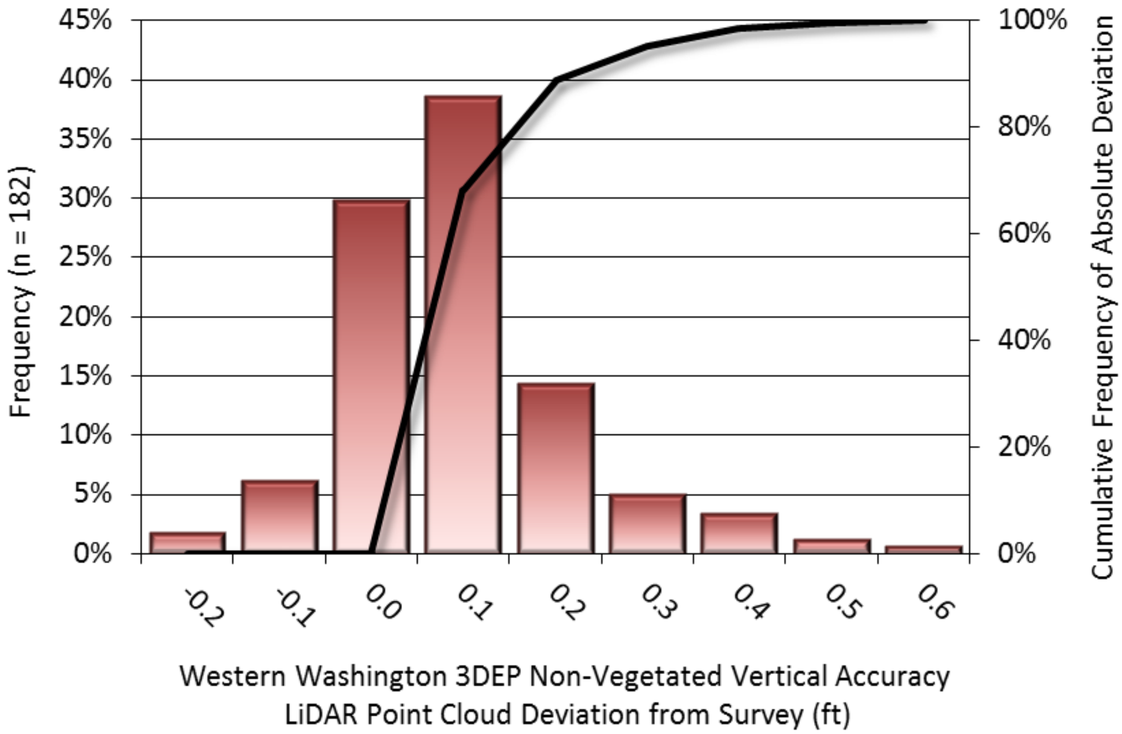

Figure 9: Frequency histogram for LiDAR unclassified point deviation from non-vegetated quality assurance point values

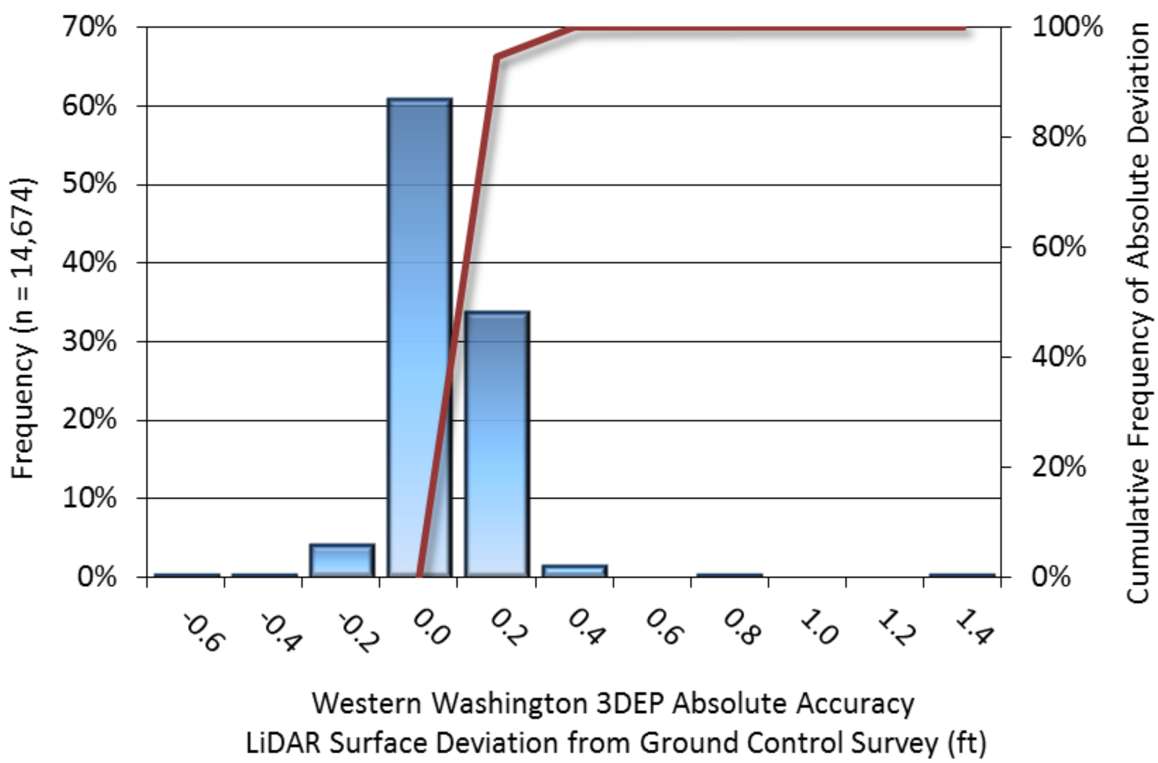

Figure 10: Frequency histogram for LiDAR surface deviation from ground control point values

LiDAR Vegetated Vertical Accuracy

QSI also assessed vertical accuracy using Vegetated Vertical Accuracy (VVA) reporting. VVA compares known ground quality assurance point data collected over vegetated surfaces using land class descriptions to the triangulated ground surface generated by the ground classified LiDAR points. For the Western Washington 3DEP survey, 115 vegetated quality assurance points tested 0.680 feet (0.207 meters) vertical accuracy at the 95th percentile (Table 13, Figure 11).

Table 13: Vegetated Vertical Accuracy for the Western Washington 3DEP Project

Vegetated Vertical Accuracy (VVA)	
Sample	115 points
Average Dz	0.215 ft 0.066 m
Median	0.199 ft 0.061 m
RMSE	0.369 ft 0.112 m
Standard Deviation (1σ)	0.301 ft 0.092 m
95th Percentile	0.680 ft 0.207 m

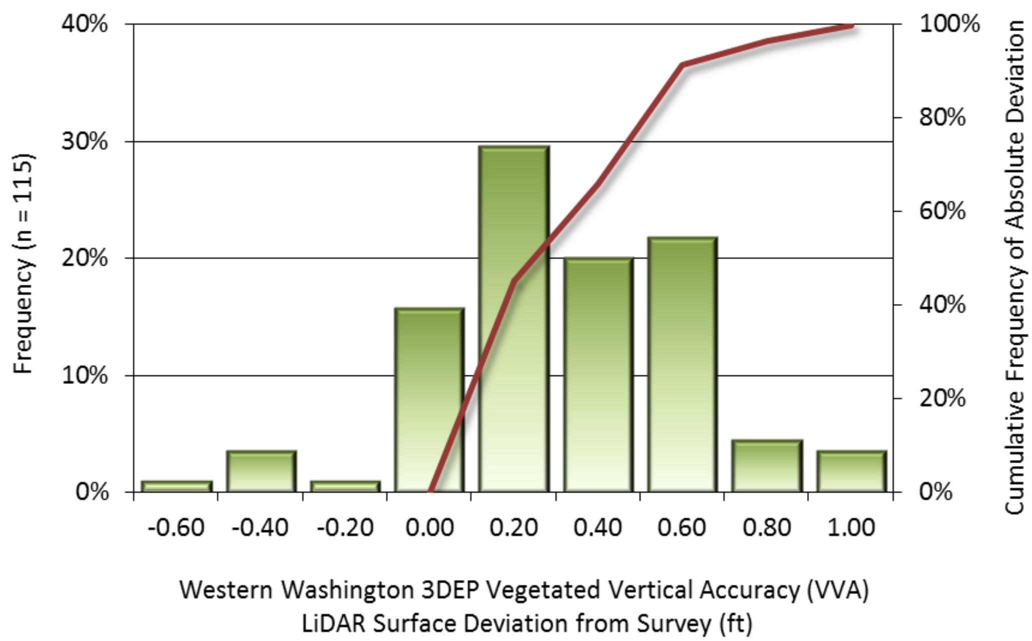

Figure 11: Frequency histogram for LiDAR surface deviation from all land cover class point values (VVA)

LiDAR Relative Vertical Accuracy

Relative vertical accuracy refers to the internal consistency of the data set as a whole: the ability to place an object in the same location given multiple flight lines, GPS conditions, and aircraft attitudes. When the LiDAR system is well calibrated, the swath-to-swath vertical divergence is low (<0.10 meters). The relative vertical accuracy was computed by comparing the ground surface model of each individual flight line with its neighbors in overlapping regions. The average (mean) line to line relative vertical accuracy for the Western Washington 3DEP LiDAR project was 0.143 feet (0.044 meters) (Table 14, Figure 12).

Table 14: Relative accuracy results

Relative Accuracy	
Sample	3,138 surfaces
Average	0.143 ft 0.044 m
Median	0.168 ft 0.051 m
RMSE	0.226 ft 0.069 m
Standard Deviation (1σ)	0.107 ft 0.033 m
1.96σ	0.209 ft 0.064 m

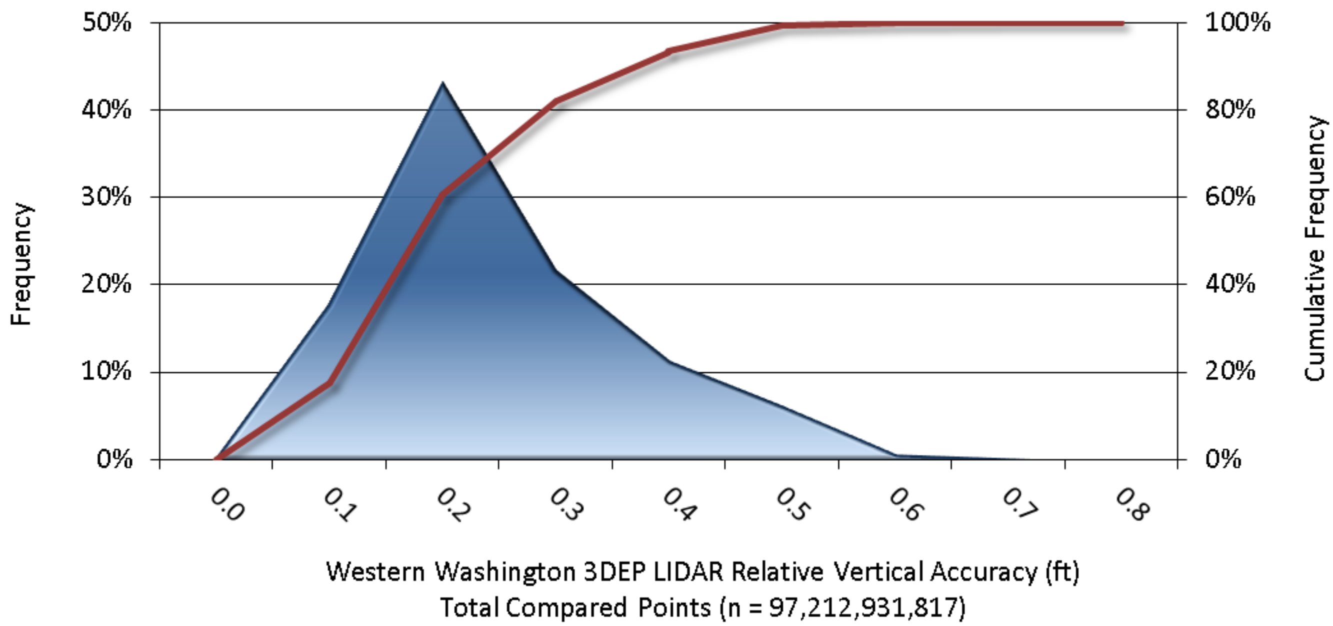

Figure 12: Frequency plot for relative vertical accuracy between flight lines

CERTIFICATIONS

Quantum Spatial, Inc. provided LiDAR services for the Western Washington 3DEP project as described in this report.

I, Tucker Selko, have reviewed the attached report for completeness and hereby state that it is a complete and accurate report of this project.

Tucker Selko
Tucker Selko (Sep 29, 2017)

Sep 29, 2017

Tucker Selko
Project Manager
Quantum Spatial, Inc.

I, Evon P. Silvia, PLS, being duly registered as a Professional Land Surveyor in and by the state of Washington, hereby certify that the methodologies, static GNSS occupations used during airborne flights, and ground survey point collection were performed using commonly accepted Standard Practices. Field work conducted for this report was conducted between March 17, 2016, and June 19, 2017.

Accuracy statistics shown in the Accuracy Section of this Report have been reviewed by me and found to meet the “National Standard for Spatial Data Accuracy”.

Evon P. Silvia

Sep 29, 2017

Evon P. Silvia, PLS
Quantum Spatial, Inc.
Corvallis, OR 97333

SELECTED IMAGES

Figure 13: This image shows a view of Anacortes, Washington, created from the bare earth and above-ground point clouds colored by elevation and overlaid with NAIP imagery.

Figure 14: This image shows a blended view of the Nooksack River and surrounding landscape, created from the bare earth DEM colored by elevation, partially overlaid with the above-ground point cloud colored using NAIP imagery.

Glossary

<u>1-sigma (σ) Absolute Deviation</u>: Value for which the data are within one standard deviation (approximately 68^{th} percentile) of a normally distributed data set.

<u>1.96 * RMSE Absolute Deviation</u>: Value for which the data are within two standard deviations (approximately 95^{th} percentile) of a normally distributed data set, based on the FGDC standards for Non-vegetated Vertical Accuracy (NVA) reporting.

<u>Accuracy</u>: The statistical comparison between known (surveyed) points and laser points. Typically measured as the standard deviation (sigma σ) and root mean square error (RMSE).

> **<u>Absolute Accuracy</u>:** The vertical accuracy of LiDAR data is described as the mean and standard deviation (sigma σ) of divergence of LiDAR point coordinates from ground survey point coordinates. To provide a sense of the model predictive power of the dataset, the root mean square error (RMSE) for vertical accuracy is also provided. These statistics assume the error distributions for x, y and z are normally distributed, and thus we also consider the skew and kurtosis of distributions when evaluating error statistics.
>
> **<u>Relative Accuracy</u>:** Relative accuracy refers to the internal consistency of the data set; i.e., the ability to place a laser point in the same location over multiple flight lines, GPS conditions and aircraft attitudes. Affected by system attitude offsets, scale and GPS/IMU drift, internal consistency is measured as the divergence between points from different flight lines within an overlapping area. Divergence is most apparent when flight lines are opposing. When the LiDAR system is well calibrated, the line-to-line divergence is low (<10 cm).
>
> **<u>Root Mean Square Error (RMSE)</u>:** A statistic used to approximate the difference between real-world points and the LiDAR points. It is calculated by squaring all the values, then taking the average of the squares and taking the square root of the average.

<u>Data Density</u>: A common measure of LiDAR resolution, measured as points per square meter.

<u>Digital Elevation Model (DEM)</u>: File or database made from surveyed points, containing elevation points over a contiguous area. Digital terrain models (DTM) and digital surface models (DSM) are types of DEMs. DTMs consist solely of the bare earth surface (ground points), while DSMs include information about all surfaces, including vegetation and man-made structures.

<u>Intensity Values</u>: The peak power ratio of the laser return to the emitted laser, calculated as a function of surface reflectivity.

<u>Nadir</u>: A single point or locus of points on the surface of the earth directly below a sensor as it progresses along its flight line.

<u>Overlap</u>: The area shared between flight lines, typically measured in percent. 100% overlap is essential to ensure complete coverage and reduce laser shadows.

<u>Pulse Rate (PR)</u>: The rate at which laser pulses are emitted from the sensor; typically measured in thousands of pulses per second (kHz).

<u>Pulse Returns</u>: For every laser pulse emitted, the number of wave forms (i.e., echoes) reflected back to the sensor. Portions of the wave form that return first are the highest element in multi-tiered surfaces such as vegetation. Portions of the wave form that return last are the lowest element in multi-tiered surfaces.

<u>Real-Time Kinematic (RTK) Survey</u>: A type of surveying conducted with a GPS base station deployed over a known monument with a radio connection to a GPS rover. Both the base station and rover receive differential GPS data and the baseline correction is solved between the two. This type of ground survey is accurate to 1.5 cm or less.

<u>Post-Processed Kinematic (PPK) Survey</u>: GPS surveying is conducted with a GPS rover collecting concurrently with a GPS base station set up over a known monument. Differential corrections and precisions for the GNSS baselines are computed and applied after the fact during processing. This type of ground survey is accurate to 1.5 cm or less.

<u>Scan Angle</u>: The angle from nadir to the edge of the scan, measured in degrees. Laser point accuracy typically decreases as scan angles increase.

<u>Native LiDAR Density</u>: The number of pulses emitted by the LiDAR system, commonly expressed as pulses per square meter.

Relative Accuracy Calibration Methodology:

Manual System Calibration: Calibration procedures for each mission require solving geometric relationships that relate measured swath-to-swath deviations to misalignments of system attitude parameters. Corrected scale, pitch, roll and heading offsets were calculated and applied to resolve misalignments. The raw divergence between lines was computed after the manual calibration was completed and reported for each survey area.

Automated Attitude Calibration: All data were tested and calibrated using TerraMatch automated sampling routines. Ground points were classified for each individual flight line and used for line-to-line testing. System misalignment offsets (pitch, roll and heading) and scale were solved for each individual mission and applied to respective mission datasets. The data from each mission were then blended when imported together to form the entire area of interest.

Automated Z Calibration: Ground points per line were used to calculate the vertical divergence between lines caused by vertical GPS drift. Automated Z calibration was the final step employed for relative accuracy calibration.

LiDAR accuracy error sources and solutions:

Type of Error	Source	Post Processing Solution
GPS (Static/Kinematic)	Long Base Lines	None
	Poor Satellite Constellation	None
	Poor Antenna Visibility	Reduce Visibility Mask
Relative Accuracy	Poor System Calibration	Recalibrate IMU and sensor offsets/settings
	Inaccurate System	None
Laser Noise	Poor Laser Timing	None
	Poor Laser Reception	None
	Poor Laser Power	None
	Irregular Laser Shape	None

Operational measures taken to improve relative accuracy:

Low Flight Altitude: Terrain following was employed to maintain a constant above ground level (AGL). Laser horizontal errors are a function of flight altitude above ground (about 1/3000th AGL flight altitude).

Focus Laser Power at narrow beam footprint: A laser return must be received by the system above a power threshold to accurately record a measurement. The strength of the laser return (i.e., intensity) is a function of laser emission power, laser footprint, flight altitude and the reflectivity of the target. While surface reflectivity cannot be controlled, laser power can be increased and low flight altitudes can be maintained.

Reduced Scan Angle: Edge-of-scan data can become inaccurate. The scan angle was reduced to a maximum of ±15-20^{o} from nadir, creating a narrow swath width and greatly reducing laser shadows from trees and buildings.

Quality GPS: Flights took place during optimal GPS conditions (e.g., 6 or more satellites and PDOP [Position Dilution of Precision] less than 3.0). Before each flight, the PDOP was determined for the survey day. During all flight times, a dual frequency DGPS base station recording at 1 second epochs was utilized and a maximum baseline length between the aircraft and the control points was less than 13 nm at all times.

Ground Survey: Ground survey point accuracy (<1.5 cm RMSE) occurs during optimal PDOP ranges and targets a minimal baseline distance of 4 miles between GPS rover and base. Robust statistics are, in part, a function of sample size (n) and distribution. Ground survey points are distributed to the extent possible throughout multiple flight lines and across the survey area.

50% Side-Lap (100% Overlap): Overlapping areas are optimized for relative accuracy testing. Laser shadowing is minimized to help increase target acquisition from multiple scan angles. Ideally, with a 50% side-lap, the nadir portion of one flight line coincides with the swath edge portion of overlapping flight lines. A minimum of 50% side-lap with terrain-followed acquisition prevents data gaps.

Opposing Flight Lines: All overlapping flight lines have opposing directions. Pitch, roll and heading errors are amplified by a factor of two relative to the adjacent flight line(s), making misalignments easier to detect and resolve.